TO:
FROM: Al Cooper
SUBJECT: Studies of the measurements of wind using LAMS

Introduction

During the 2015 ARISTO project on the C-130, the LAMS was flown in a 4-beam configuration. The beam assignments were non-standard, though, with beam 2 forward, beam 1 downward, beam 3 outboard and upward, and beam 4 inboard and upward. Beams 1, 3 and 4 were approximately 35° from the forward direction, and relative to an azimuthal angle starting from the downward direction they were, respectively, 0, −120 and 120° in clockwise rotation about the forward longitudinal axis.

There were five research flights. All had some degree of measurement problems, so data for this study have been selected from the periods that appear to provide the best measurements. The following table provides a few of the characteristics of these flights:

date	start	end	profile	problems
150916	160225	200605	climb->20kft, level, stepped descent to BL, no maneuvers	LAMS IRU attitude angles bad
150923	135907	204016	mostly low level until near end; LAMS reasonable, although weak; some speed variations	actual takeoff about 170000; BEAM2speed weak, BEAM2_LAMS (Scott's value) better.
150925	162500	214500	both upper and lower-level legs; speed runs, pitch maneuvers, some turbulence	CPITCH_LAMS bad before 192300, and CROLL also, so wind measurements from LAMS unavailable until after then.
150930	170100	205000	good pitch and yaw maneuvers; also a partial speed run.	Beams 1 and 4 problematic before 1915 in high-level leg; beam 2 probably useful for TAS.
151002	143000	184400	upper-level pitches and lower-level turbulence	LAMS beam peaks look very weak to me, questionable although SMS processing seems reasonable.

The line-of-sight beam speeds were determined in two ways. Scott Spuler used principal-component analysis to find the beam speeds, and usually this worked very well, although there are some suspicious times. For example, the peaks in Flight 5 look very weak, yet the PCA method continued

to find output values. Because there was tight coupling to the expected measured TAS (with adjustment for the beam angles), it appears suspicious that the method may be duplicating the TAS value at times without having an adequate signal. The match to TASX looks so good that it seems suspicious, as discussed later. A second method was to fit the background using Savitzgy-Golay polynomials and then search for peaks above this background. When signals were strong, the method usually produced the same result as the PCA method, but it was more prone to failure during periods where the signal was weak. (A signal-to-noise test of ≥ 4 was required for a valid measurement.) Results from both these peak-detecting algorithms will be discussed in this memo.

There are several objectives that can be met by using the LAMS-derived measurements:

1. The LAMS provides an independent measurement of angle-of-attack and sideslip angle, so these measurements can be used to check the empirical relationships used to calibrate the radome-based measurements of these angles.

2. LAMS provides an independent measurement of the airspeed, so from that measurement it is possible to determine the expected dynamic pressure. This was used previously(Cooper et al., 2014) to calibrate not only the dynamic pressure but also the static pressure as measured on the C-130. However, since then the offset between the avionic static pressure and the research static pressure calibrated in this way has changed, so it is important to learn if the static defect actually changed or perhaps the avionic value changed. This has an important effect on the longitudinal component of the measured wind as well.

3. The method used to calibrate the radome is based primarily on slowly varying measurements, such as the variation in angle-of-attack during a speed run. It is of concern that the calibration used might not apply in the case of rapidly changing flight conditions, when for example there might be transient adjustment of the airflow pattern toward a new steady state. Because the LAMS measures wind well ahead of the aircraft, such effects should not appear in the LAMS-based measurements, so a comparison of the LAMS-based and radome-based measurements might either identify transient-response problems or place limits on how large such effects might be.

Data processing

The original netCDF files, with names like ARISTOrf01.nc, contain histograms of the LAMS frequency measurements, with names like BEAM{1–4}_LAMS. Scott Spuler has processed these to produce files like ARISTOrf01_LAMS.nc with new variables Beam{1–4}_LAMS containing the line-of-sight speeds measured in each beam. In addition, the Python program LAMS_ARISTO.py has been used to process these further to files ARISTOrfxx_LAMSLAMS.nc, which contain additional variables BEAM{1–4}speed also representing the line-of-sight speeds. Both sets of variables, Beam{1–4}_LAMS and BEAM{1–4}speed, will be used, but they appear to have different strengths:

1. The variables Beam{1–4}_LAMS are produced by Spuler's PCA routine. This is the most sensitive detection method, but there is some suspicion that it produces values when there is inadequate signal, perhaps by too much reliance on TASX to determine where the peak should be.

2. The variables BEAM{1–4}speed are produced by smoothing the histograms with Savitzgy-Golay polynomials and then searching for peaks above the smoothed background. This algorithm also uses TASX to determine likely locations for the peaks, but with a fairly large tolerance, and it requires a signal-to-noise ratio ≥ 4 or else it produces a missing-value result. In ARISTO2015, this algorithm was significantly less sensitive than the PCA algorithm, and for example in Flight 5 it mostly did not produce useful results while the PCA algorithm produced almost continuous results for the line-of-sight beam speeds.

The Python routine also produced new variables named WD_LAMS, WS_LAMS, WI_LAMS, ATTACK_L and SSLIP_L, using the processing algorithms for a 4-beam LAMS that were discussed in the documents LAMSprocessing4Bwind.pdf and LAMSprocessing3Dwind.pdf. These variables were also used in the present R routine (this file) to generate measurements of vertical and horizontal wind, airspeed, and angles of attack and sideslip. For airspeed, angle of attack, and sideslip, these steps were used:

1. The four-beam measurements were used to determine a three-dimensional relative wind vector **RW**=$\{\mathrm{RW}_x, \mathrm{RW}_y, \mathrm{RW}_z\}$ with components inbound along the longitudinal forward, lateral starboard, and lateral downward axis in the coordinate frame of the LAMS IRU (with attitude angles CPITCH, CROLL, CTHDG). The algorithm is documented in LAMSprocessing4Bwind.pdf.

2. The airspeed is then the magnitude of the vector **RW**.

3. The angle of attack is $\alpha = \arctan(\mathrm{RW}_z/\mathrm{RW}_x)$ and the sideslip angle is $\beta = \arctan(\mathrm{RW}_y/\mathrm{RW}_x)$.

The results for the various processing schemes are shown in Fig. 1.

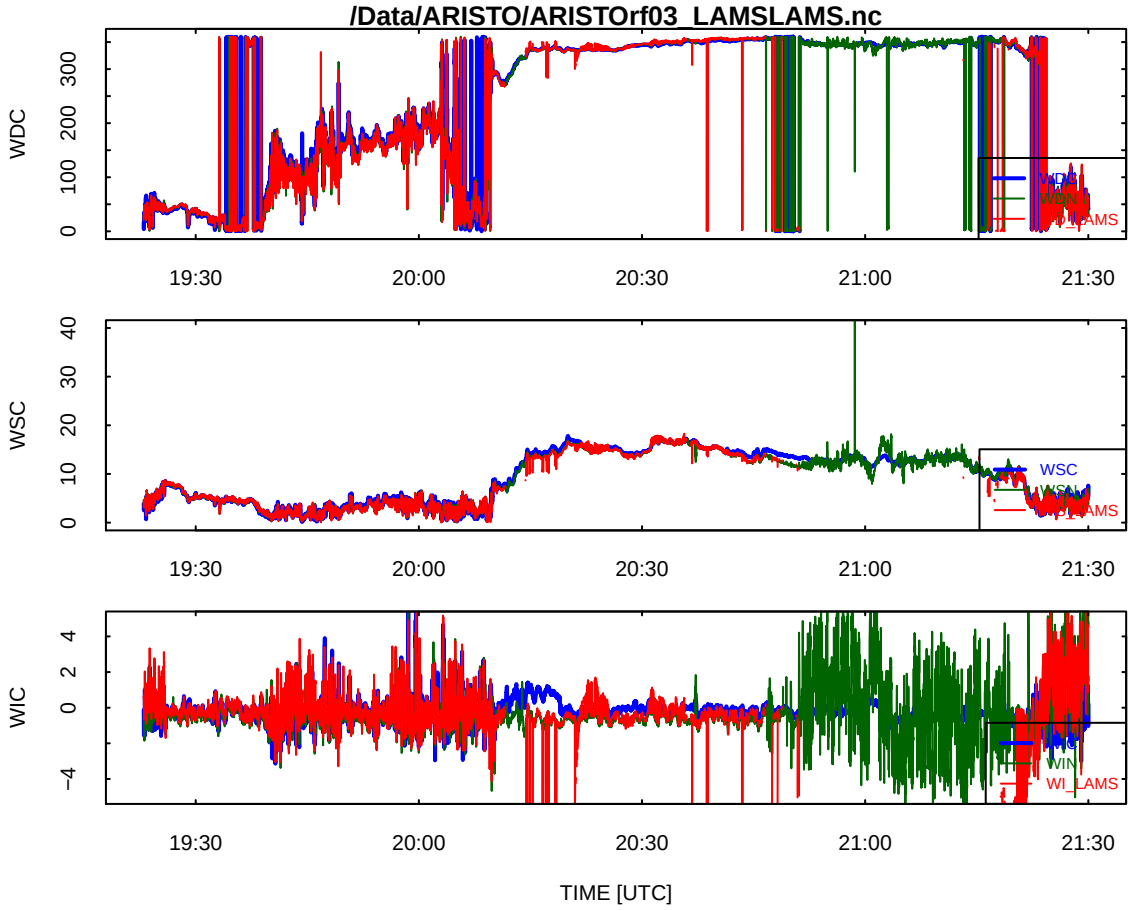

Figure 1: Wind measurements: conventional (blue), PCA-based (green), SG-based (red). The time period is restricted to 19:23–21:30 UTC because the LAMS IRU produced erronous values for the attitude angles at other times.

Sensitivity coefficients

Angle of attack

The following speed-run maneuvers are available from ARISTO2015:

#	flight	start	end	comments
1	2	183200	185500	PCA, not SG
2	2	192100	193800	PCA or (SG exc 193000)
3	3	171300	173800	CPITCH bad
4	3	183400	185700	CPITCH bad
5	3	205500	210000	slowdown only; PCA only
6	4	174300	180700	PCA only
7	4	191200	193000	PCA only; SG weak
8	4	202500	203900	PCA; SG B1 weak

The values of vertical wind as originally processed did not look very good, so the first step was to determine a conventional set of sensitivity coefficients to use as a radome calibration. For this purpose, a data.frame consisting of a concatenation of the eight speed runs in the preceding table was constructed and a reference value for calibration (AOAREF) was added to the data.frame. AOAREF, defined below, is the value that should be measured for angle of attack if the true vertical wind is zero during the maneuver:

$$\mathrm{AOAREF} = \theta + \frac{w_p}{V}\frac{180}{\pi}$$

where θ is the pitch angle (variable PITCH), w_p is the rate of climb of the aircraft (variable GGVSPD), and V is the true airspeed (variable TASX). The conventional fit is then

$$\mathrm{AOAREF} = c_0 + \frac{\mathrm{ADIFR}}{\mathrm{QCF}}\left(c_1 + c_2\,\mathrm{MACH}\right)$$

where MACH is the Mach number determined from the uncorrected measurements PSFD and QCF (cf. the technical note on processing algorithms). In addition, a data.frame consisting of all measurements from flights 2–4 was constructed and coefficients were also determined for a fit to those data.

Figure 2 shows the resulting fit, with coefficients $\{c_0, c_1, c_2\}$ = {4.7314, 11.5015, 3.0546}. However, the results differed for the three flights, and the differences were significant, as shown in the following table:

Flight	c_0	c_1	c_2
speed runs	4.7314	11.5015	3.0546
all rf02–04	4.6298	11.7147	1.5477
2	4.1623	6.0555	13.9073
3	4.5892	8.4874	8.5789
4	4.9885	12.4355	2.0626

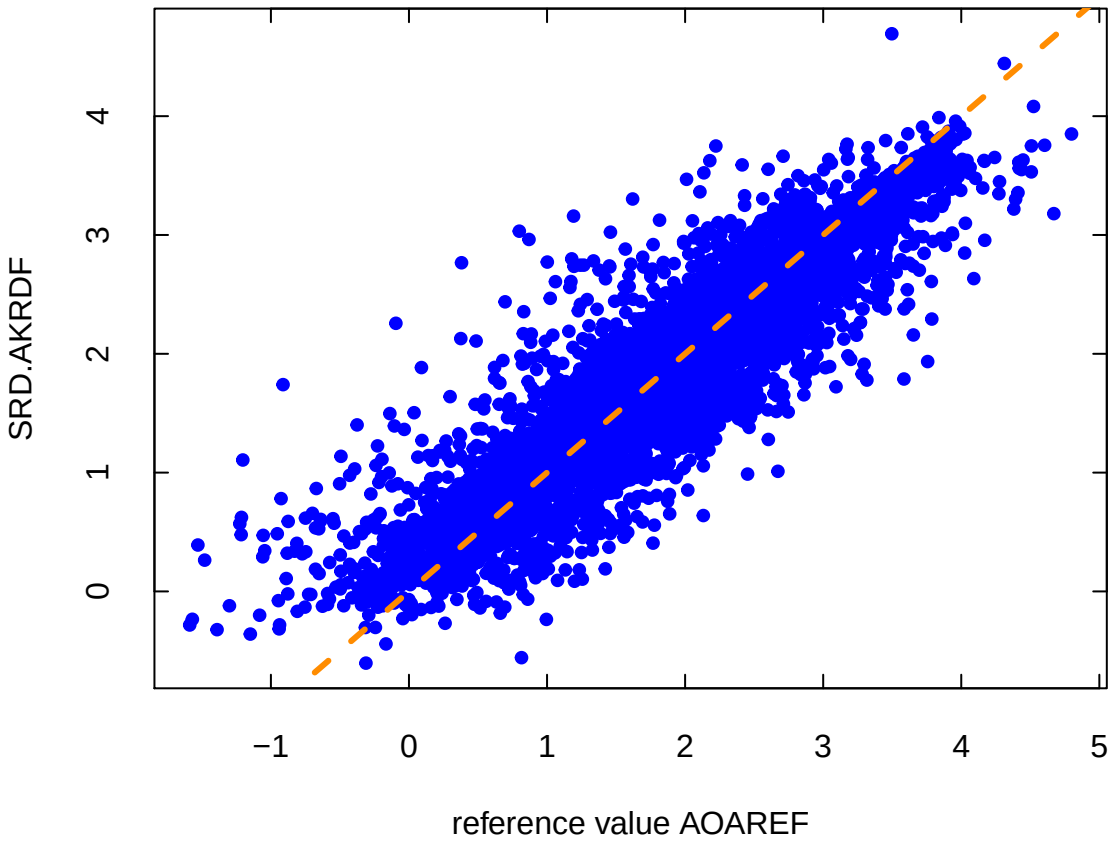

Figure 2: Angle of attack from the new calibration vs. the corresponding value of the reference variable AOAREF.

Therefore, the individual-flight coefficients will be used to determine AKRD and hence WIC in the following studies in this report.

An additional adjustment of the measurements is useful because the LAMS is not installed parallel to the centerline of the aircraft. For example, the average measurement of pitch from the LAMS IRU, CPITCH_LAMS, is 1.0° larger than the corresponding measurement of pitch from the Honeywell IRU. To account for this offset, it is useful to correct both the pitch and angle-of-attack from LAMS by the subtraction of 1.0° so that the measurements will be comparable to those from the standard radome-based system. That correction has been made in the following when the LAMS-based angle-of-attack is discussed.

With these corrections, the standard angle-of-attack can be compared to that determined from the LAMS. The first speed run in the table above will be skipped here because there are too many bad measurements from LAMS. For the second speed run, Figure 3 shows the comparison of the two angles of attack. There is a clear difference between the two measurements. Speed runs #3 and #5

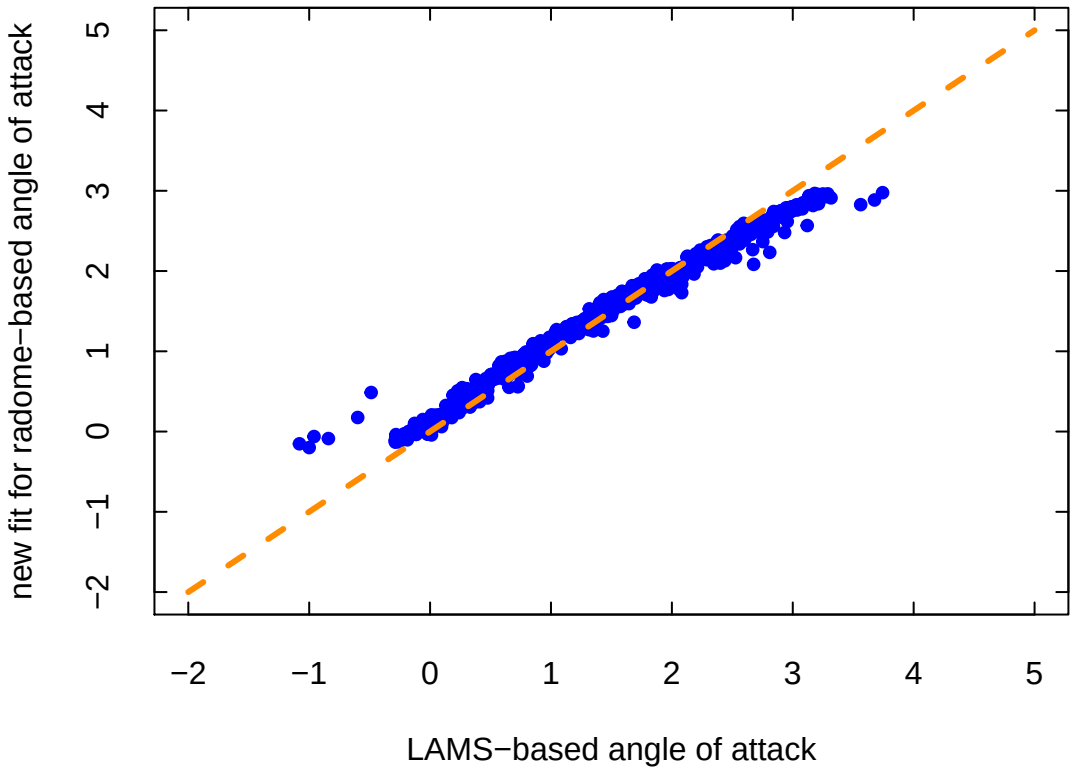

Figure 3: Angle of attack from the new fit to the radome values, plotted against the corresponding anagle-of-attack as measured by the LAMS, for speed run #2.

have too much scatter in the LAMS measurements to be useful, but speed run #4 has apparently good measurements as shown in Fig. 4. Here the scatter is much higher than in Fig. 3 because this is a low-level flight segment in boundary-layer turbulence, but the measurements still show an offset like that in Fig. 3, although perhaps with a smaller offset. Speed runs #6 and #8 have high scatter and are inconsistent with other apparently good speed runs, but speed run #7 led to good agreement between the values of the radome-based and LAMS-based angles of attack, as shown in Fig. 5.

Figures 3 and 5 show reasonable consistency between the two measurements, while there is a significant offset evident in Fig. 4. Because speed run #4 is a low-level boundary-layer leg, there may be bias introduced by the proximity of the ground and strong reflection from it that could affect the downward-pointing beam. A fit to the radome-based angle of attack as a function of the LAMS-based value gave regression coefficients of 0.66 (offset) and 0.70 (slope), so these measurements are clearly inconsistent.

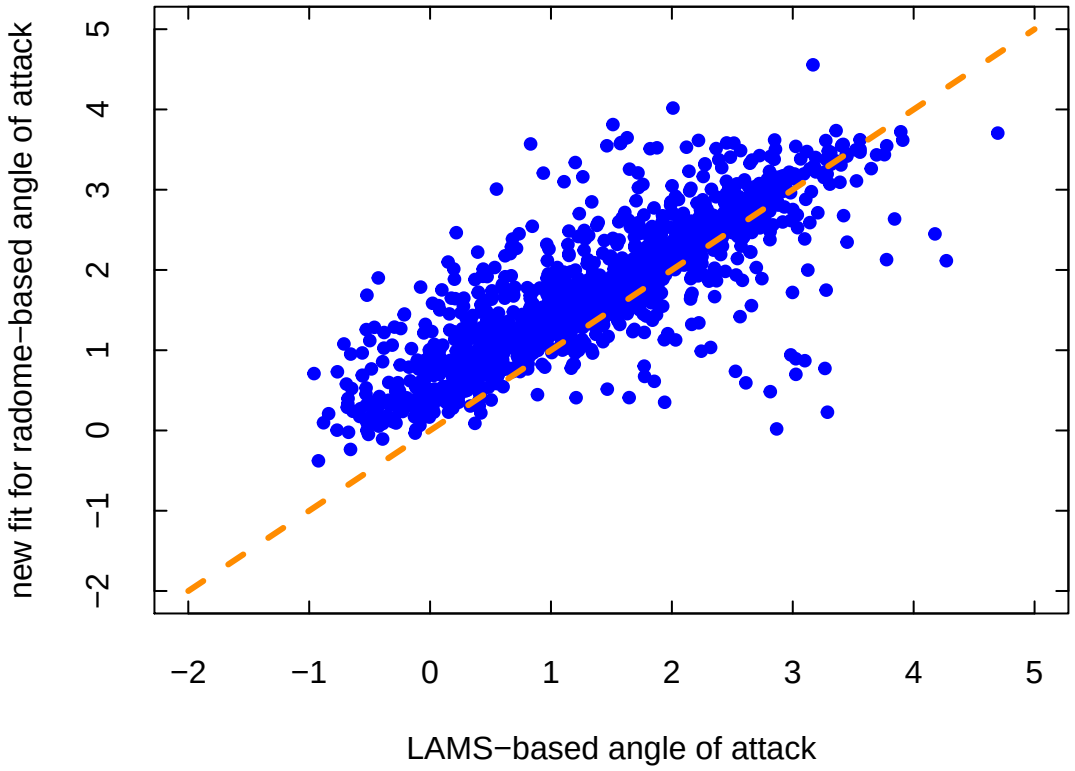

Figure 4: Angle of attack from the new fit to the radome values, plotted against the corresponding anagle-of-attack as measured by the LAMS, for speed run #4.

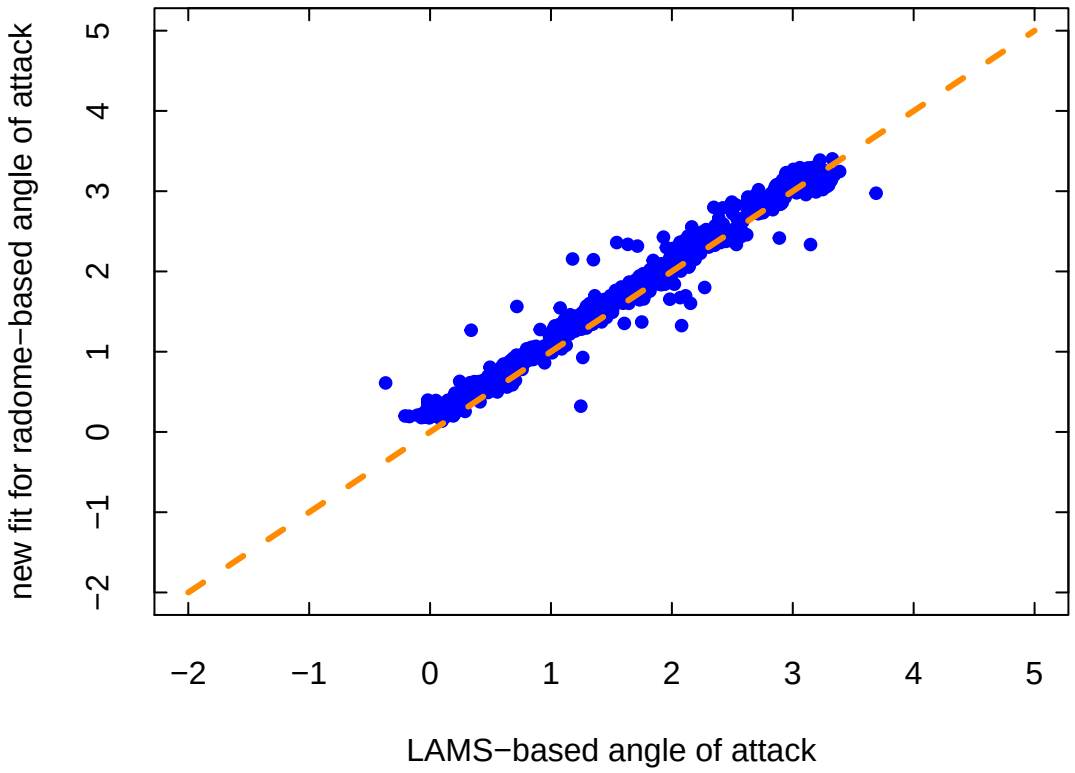

Figure 5: Angle of attack from the new fit to the radome values, plotted against the corresponding anagle-of-attack as measured by the LAMS, for speed run #7. Some additional outlier points having difference between the measurements larger than 1 degree have been excluded from the plot.

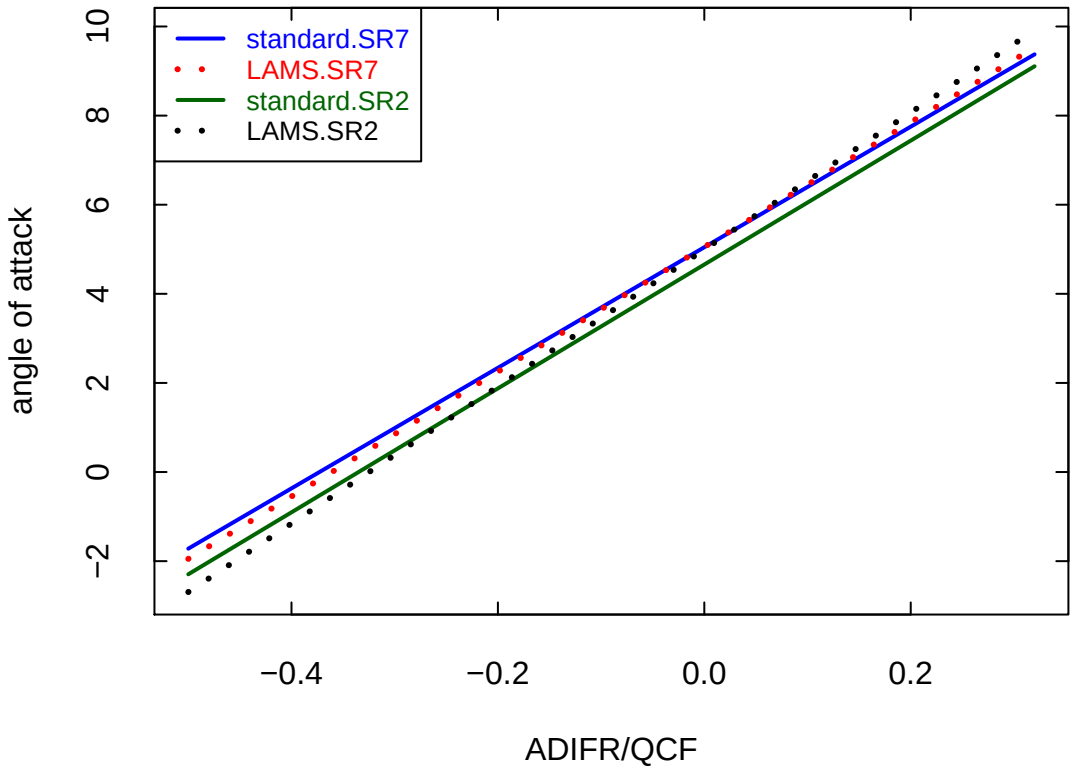

Figure 6: Comparison of the standard and LAMS-based calibrations for speed run #7.

A revised LAMS-based calibration for the radome sensitivity coefficients can then be determined by using the LAMS-based angle of attack as the reference for the fits. Separate fits for speed-run #2 and for #7 produced significantly different results, so both the conventional and LAMS-based calibrations differ for the two speed runs. The following table summarizes the results:

speed run	**source of calibration**	c_0	c_1	c_2
#2	AOAREF	4.6576	13.9045	0
#2	LAMS ATTACK	4.9945	15.3775	0
#7	AOAREF	5.0451	13.5299	0
#7	LAMS ATTACK	5.0512	13.9997	0
#2+#7	LAMS ATTACK	4.6694	9.7585	8.4181

The four calibrations in the preceding table are plotted in Fig. 6. For speed run #7, the calibrations based on LAMS and on AOAREF are close to the same, although there are small differences of typical magnitude of about 0.1°for angles-of-attack in the typical range of operations (0–4°).

However, the different calibrations for speed run #2 are not as consistent, and both calibrations differ significantly from those for speed run #7. For the conventional calibration, this might be attributed to a non-zero vertical wind during the calibration maneuver, but the LAMS calibration is not affected by the vertical wind so it should be definitive unless there was some problem with detection of the LAMS beams. Another possibility is drift of the CPITCH_LAMS measurement, but the difference between PITCH and CPITCH_LAMS is the same for speed run #2 as for speed run #7.

The result is that the two best speed runs, #2 and #7, are inconsistent. Calibrations for speed run #7 support the validity of each, but there is larger than expected difference between the two calibrations for #2 and between the corresponding calibrations for #7 vs #2. These are the best calibration data available, so more measurements with adequate LAMS signal-to-noise would be valuable. Pending such measurements, the LAMS-based calibration for #7 may be the most reliable.

Another conclusion from the study of the speed runs is that the PCA analysis does not always produce reliable line-of-sight speeds. A good example is speed run #6. There are values for all four beam line-of-sight speeds through this maneuver, and the speed in the forward beam (Beam 2) matches the true airspeed (TASX) well. However, Fig. 7 shows that the angle-of-attack determined from these measurements does not match that determined from the radome-based system and looks very noisy. This raises a warning that sometimes the line-of-sight speeds are not valid even when the PCA algorithm detects peak values.

Sideslip angle

There were four yaw maneuvers that can be used to find the sensitivity coefficients for the sideslip measurement, as listed in the following table:

maneuver #	flight	start	end
1	2	194100	194330
2	4	182800	183100
3	4	190130	190400
4	4	201830	202130

First, for completeness, the conventional fit will be used:

$$\beta^* = -\Psi + \arctan\frac{u_p - u}{v_p - v}$$

where β^* is the reference value for the fit, Ψ is the heading, u_p and v_p the eastward and northward components of the aircraft ground-speed and u and v are the east and north components of the wind. The empirical relationship for sideslip then can be found by fitting for the coefficients $\{s_0, s_1\}$ in:

$$\beta^* = b_0 + b_1\frac{\mathrm{BDIFR}}{\mathrm{QCXC}}$$

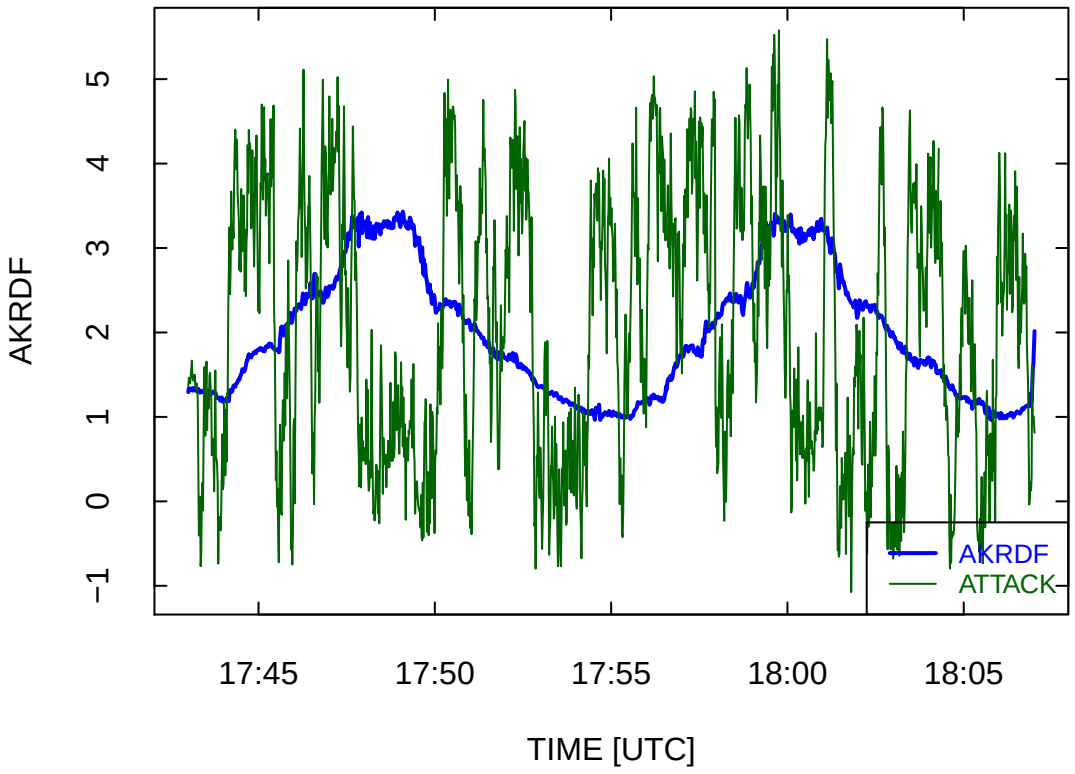

Figure 7: Angle of attack from the new fit to the radome values (blue line) and the angle-of-attack determined from the LAMS measurements (green line), for speed run #6.

and then finding the sideslip angle from

$$\mathrm{SSRD} = b_0 + b_1 \frac{\mathrm{BDIFR}}{\mathrm{QCXC}} \ .$$

Figure 8 shows that the resulting values for SSRD are in close correspondence to the reference values for the four combined yaw maneuvers.

The resulting sensitivity coefficients for sideslip are $\{b_0, b_1\} = \{1.5478,\ 12.6582\}$. The fit was very good, with a residual standard deviation of 0.12°. For comparison, the standard values in the Technical Note on Processing Algorithms are $\{0,\ 12.2115\}$. As discussed in the Technical Note on Wind Uncertainty, it is difficult to separate an offset in sideslip from an offset in heading, so the difference in the first coefficient may instead apply to heading.[1] The difference in offsets for these two calibrations is large, although the slope coefficients are in reasonable agreement.

[1] An offset of -0.1° applied to heading in the original processing has not been removed here.

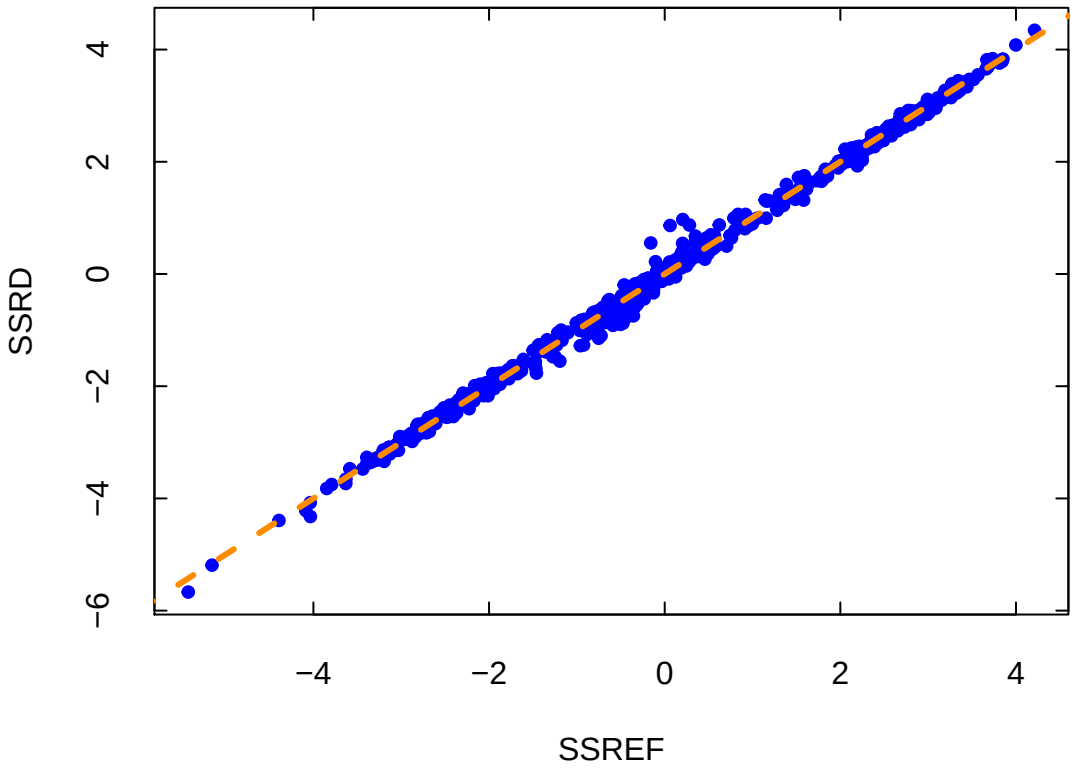

Figure 8: Sideslip angle calculated using new fit coefficients (SSRD) as a function of the reference value for sideslip (SSREF). The relationship determined by regression is shown as the dashed orange line.

The LAMS measurement of sideslip provides an alternate means of determining the slope parameter.[2] The reference value β^* for the fit can be determined from the LAMS-based measurements of the relative wind, as discussed in the introductory section:

$$\beta^* = \arctan\left(\frac{\mathrm{RW}_y}{\mathrm{RW}_x}\right)$$

The LAMS-based measurements of sideslip bear little similarity to those from the radome for sideslip maneuvers #2 and #3, so there are evidently measurement problems that make those unreliable. Maneuver #4 is good, and maneuver #1 appears valid for the period 194130–194305, so those measurements were used for the fit. The LAMS-based fit gave coefficients $\{b_0, b_1\} = \{1.5995, 12.3612\}$, with a residual standard deviation about the fit of 0.13°. These values are close

[2]The appropriate offsets in sideslip and heading will still need to be found from analysis of circle maneuvers.

to those determined in the standard way, so this calibration provides support for the conventional approach, although the difference in slope is significant (with estimated standard uncertainty in b_1 of 0.05°). The value for b_1 determined from the LAMS-based measurements, 12.36°, appears to be the best available, but the value of b_0 still needs to be determined from the circle maneuvers that can separate an offset in sideslip from an offset in heading.

– End of Memo –

Reproducibility:

PROJECT:	ARISTO2015-LAMS
ARCHIVE PACKAGE:	ARISTO2015-LAMS.zip
CONTAINS:	attachment list below
PROGRAM:	ARISTO2015-LAMS.Rnw
ORIGINAL DATA:	
WORKFLOW:	WorkflowARISTO2015-LAMS.pdf
GIT:	https://github.com/WilliamCooper/ARISTO2015-LAMS.git

Attachments: ARISTO2015-LAMS.Rnw
ARISTO2015-LAMS.pdf
ARISTO2015-LAMS.Rdata.gz
SessionInfo